This article has been accepted for publication in a future issue of this journal, but has not been fully edited. Content may change prior to final publication. Citation information: DOI 10.1109/TCOMM.2015.2512603, IEEE Transactions on Communications

Suppressing Alignment: Joint PAPR and Out-of-Band Power Leakage Reduction for OFDM-Based Systems

Anas Tom[1], *Student Member, IEEE,* Alphan Şahin[1], *Member, IEEE*, and Hüseyin Arslan[1,2], *Fellow, IEEE*
[1]Department of Electrical Engineering, University of South Florida, Tampa, FL, 33620
[2]College of Engineering, İstanbul Medipol University, Beykoz, İstanbul, 34810
Email: atom@mail.usf.edu, alphan@mail.usf.edu, arslan@usf.edu

***Abstract*—Orthogonal frequency division multiplexing (OFDM) inherently suffers from two major drawbacks: high out-of-band (OOB) power leakage and high peak-to-average power ratio (PAPR). This paper proposes a novel approach called *suppressing alignment* for the joint reduction of the OOB power leakage and PAPR. The proposed approach exploits the temporal degrees of freedom provided by the cyclic prefix (CP), a necessary redundancy in OFDM systems, to generate a suppressing signal, that when added to the OFDM symbol, results in marked reduction in both the OOB power leakage and PAPR. Additionally, and in order to not cause any interference to the information data carried by the OFDM symbol, the proposed approach utilizes the wireless channel to perfectly align the suppressing signal with the CP duration at the OFDM receiver. Essentially, maintaining a bit error rate (BER) performance similar to legacy OFDM without requiring any change in the receiver structure.**

***Index Terms*—Interference alignment, out-of-band power leakage, peak-to-average power ratio, sidelobe suppression, spectrum shaping.**

I. Introduction

Orthogonal frequency division multiplexing (OFDM) is widely regarded as the multicarrier transmission of choice used in most of the existing broadband communication standards, e.g., WiFi, WiMAX, LTE, and IEEE 802.22 WRAN. This prevalent adoption of OFDM is due to its numerous advantages such as high spectral efficiency, tolerance to multipath fading, waveform agility, and simple equalization. However, despite all these attractive features, OFDM suffers from two major drawbacks: 1) out-of-band (OOB) power leakage as a result of its high spectral sidelobes and 2) high peak-to-average power ratio (PAPR). Both of these shortcomings have a large impact on the performance of OFDM and can greatly limit its practical applications. For example, the high spectral sidelobes, if not treated, can create severe interference to users operating in adjacent channels [1]. The high spectral sidelobes are caused primarily because of the inherent use of rectangular pulse shaping in the generation of OFDM, which behaves as a sinc function in the frequency domain with a spectrum that decays as f^{-2} [2]. In addition to the high spectral sidelobes, high PAPR is another problem that is common to all multicarrier transmission schemes including OFDM. The PAPR problem arises from the fact that OFDM signals are composed of multiple subcarriers with independent amplitudes and phases, that when added together, are more likely to generate a signal with high peak power [3]. Such peak power may lead to the signal being severely clipped, especially if it exceeds the linear region of operation of the transmitter power amplifier (PA). Signal clipping creates serious inband distortion that ultimately results in large degradation in the bit error rate (BER) performance at the receiver. Besides the inband distortion, high PAPR leads also to spectral spreading, commonly referred to as OOB spectral regrowth [4].

Both problems received great attention from the research community, where multiple algorithms were proposed that address the two problems either separately such as [5]–[19] for OOB radiation reduction, [3], [20] and the references therein for PAPR reduction, or jointly in [21]–[23]. Among the OOB reduction techniques, traditional time domain windowing and its variations [5]–[7] are considered as a simple and effective way of suppressing the spectral sidelobes, where an extended guard interval is added to the OFDM symbol to smooth the transitions between successive symbols. However, despite their simplicity, windowing algorithms reduce the spectral efficiency, especially when the added guard interval is large. Another class of algorithms that are also very useful in reducing the power leakage based on the use of cancellation subcarriers are proposed in [8]–[11]. There, a subset of subcarriers, modulated with optimized complex weights, are reserved primarily for suppressing the spectral sidelobes of the transmitted signal. However, just like time domain windowing, cancellation algorithms also reduce the transmission rate since the reserved subcarriers are essentially dummy tones that do not carry any data information. More advanced techniques such as precoding are reported in [12]–[19]. In general, precoding schemes produce significant reduction in the OOB leakage compared to other state of the art algorithms, but they also have their own limitations. For example, the non-orthogonal precoders in [12]–[14], [18] destroy the orthogonality between the OFDM subcarriers and therefore result in error performance degradation at the receiver. On the other hand, the orthogonal precoders in [15]–[17], [19], while all are able to maintain the same error performance as plain OFDM,

Part of this work has been submitted to ICC 2015 in London.

This article has been accepted for publication in a future issue of this journal, but has not been fully edited. Content may change prior to final publication. Citation information: DOI 10.1109/TCOMM.2015.2512603, IEEE Transactions on Communications

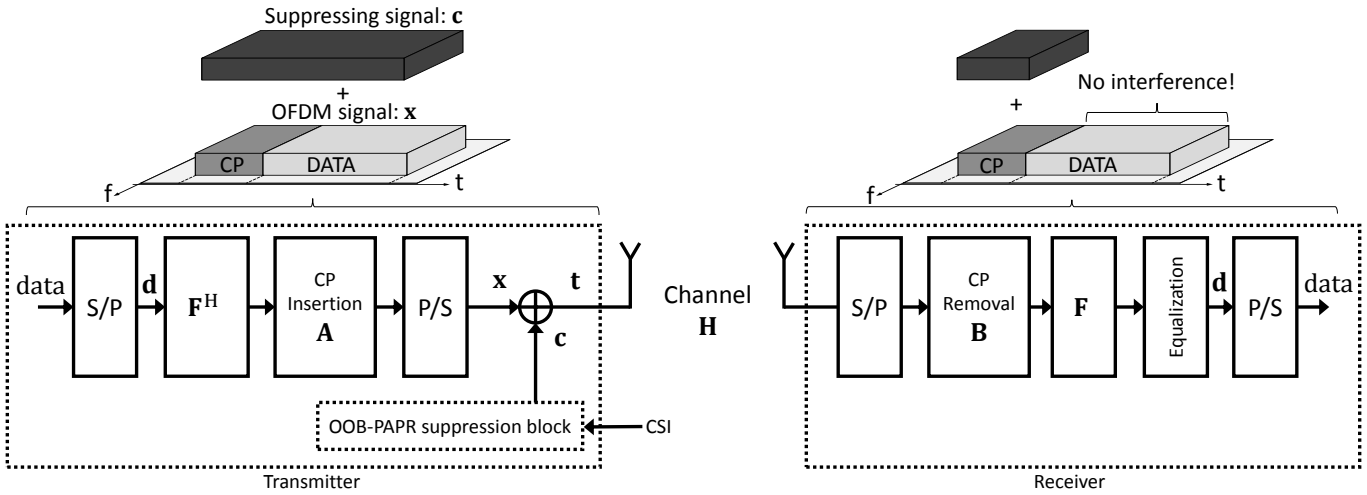

Fig. 1: System model of an OFDM transmitter and receiver with suppressing alignment.

they do so by sacrificing the spectral efficiency.

Almost all existing solutions for the OOB leakage reduction suffer from either a spectral efficiency loss or BER degradation. Furthermore, all of the aforementioned spectral suppression algorithms ignore the issue of high PAPR, an inherent characteristic of OFDM waveforms. As a result, the gains in OOB leakage reduction provided by these algorithms might be misleading, i.e., the spectral sidelobes can potentially grow back up after the high peak power transmitted signal passes through the PA. Therefore, and for the reasons outlined above, particularly the spectral regrowth problem, we believe that the best way is to address the two problems jointly as done in [21]–[24]. Following this path, we herein propose a novel algorithm, that we call *suppressing alignment*, for the joint suppression of both the OOB leakage and PAPR without any reduction in the transmission rate. Our algorithm exploits the temporal degrees of freedom provided by the cyclic prefix (CP), a necessary redundancy in OFDM systems, to properly design a suppressing signal that can effectively reduce both the OOB power leakage and PAPR of the OFDM signal. In particular, our approach adds another dimension to the use of the CP. Traditionally, the CP has been exploited mainly to mitigate the impact of inter-symbol interference (ISI) in multipath fading channels. In this work, we extend that functionality by also utilizing the CP for the purpose of spectral emissions suppression and PAPR reduction. Besides exploiting the CP, our design also utilizes the wireless channel to align the generated suppressing signal with the CP duration of the OFDM symbol at the receiver. By doing so, the suppressing signal will not cause any interference to the data portion of the OFDM symbol. From an interference point of view, the data carried in the OFDM symbol appears to be corrupted by the suppressing signal at the transmitter. However, after passing through the channel, the suppressing signal is perfectly aligned with the CP. In light of such alignment, the data portion of the OFDM symbol appears completely free of interference to the receiver. Thus, after discarding both the CP and the aligned suppressing signal through a simple CP removal operation, the receiver can decode the data with an error performance similar to that of standard OFDM. In addition to maintaining a spectral efficiency and error performance similar to plain OFDM, another advantage of our approach is that it does not require any change in the receiver structure of legacy OFDM.

Similar approaches, albeit for different purposes, have previously been proposed in [25] for interference alignment in two-tierd networks, in [26] for improving the secrecy rate of OFDM systems, and very recently in [27] for energy harvesting. Nevertheless, we believe that this is the first approach that exploits such a design for the purpose of spectral emissions and PAPR containment.

The rest of the paper is organized as follows. In Section II, the system model is introduced. The concept of suppressing alignment and its application to the reduction of OOB leakage is presented in Section III. The joint reduction of OOB leakage and PAPR is presented in Section IV. We discuss the practical implementation issues of the proposed approach is Section V. In Section VI, we provide the numerical results and finally the conclusion is provided in Section VII.

Notations: $\mathbf{I}_N$ is the $N \times N$ identity matrix; $\mathbf{0}_{N\times M}$ is an all zeros $N \times M$ matrix. The transpose and conjugate transpose are denoted by $(\cdot)^{\mathrm{T}}$ and $(\cdot)^{\mathrm{H}}$, respectively. $\|\cdot\|_2$ denotes the 2-norm and $\|\cdot\|_\infty$ denotes the uniform norm. $\mathbb{E}[\cdot]$ denotes the expectation operator while $\ker(\cdot)$ denotes the kernel of the matrix. The field of real and field of complex numbers are represented by $\mathbb{R}$ and $\mathbb{C}$, respectively. $\mathcal{CN}(\mu, \Sigma)$ is the complex Gaussian distribution with mean μ and covariance matrix Σ.

II. System Model

We consider a single link OFDM system consisting of a transmitter and a receiver communicating over a Rayleigh multipath channel as shown in Fig. 1. For ease of analysis and without any loss of generality, we assume an adjacent user, employing OFDM or any other technology, operating over a bandwidth spanning K subcarriers within the transmission band of the OFDM system. Therefore, the OFDM transmitter/receiver pair should control their transmissions such that minimal interference is caused to this adjacent user. Let the total number of

This article has been accepted for publication in a future issue of this journal, but has not been fully edited. Content may change prior to final publication. Citation information: DOI 10.1109/TCOMM.2015.2512603, IEEE Transactions on Communications

subcarriers be N, where the subcarriers spanning the adjacent user band, i.e., $\{i+1, ..., i+K\}$, are deactivated. The remaining N_d active subcarriers $\{1, ..., i\} \cup \{i+K+1, ..., N-1\}$, whereas the DC subcarrier is disabled, are modulated by a set of QAM symbols contained in a vector $\mathbf{d} \in \mathbb{C}^{N_d \times 1}$. To mitigate the effects of ISI, a CP of length L samples, which is assumed to be larger than the maximum delay spread of the channel, is added to the start of the OFDM symbol. The resulting time domain OFDM signal is expressed in vectorized form as

$$\mathbf{x} = [x_1, ..., x_{N+L}]^{\mathrm{T}} = \mathbf{A}\mathbf{F}^{\mathrm{H}}\mathbf{M}\mathbf{d} \ , \tag{1}$$

where $\mathbf{F}$ is the N-point discrete Fourier transformation (DFT) matrix, $\mathbf{M} \in \mathbb{R}^{N \times N_d}$ is a subcarrier mapping matrix containing the N_d columns of $\mathbf{I}_N$ corresponding to the active data subcarriers and $\mathbf{A} \in \mathbb{R}^{(N+L)\times N}$ is the CP insertion matrix defined as

$$\mathbf{A} = \begin{bmatrix} \mathbf{0}_{L \times N-L} & \mathbf{I}_L \\ & \mathbf{I}_N \end{bmatrix} \ .$$

To control the spectral emissions of the transmitted signal as well as its PAPR, the OOB-PAPR suppression block generates a time-domain *suppressing signal* $\mathbf{c} = [c_1, ..., c_{N+L}]^{\mathrm{T}}$ with the same length as the OFDM signal, i.e., $\mathbf{c} \in \mathbb{C}^{(N+L)\times 1}$. Furthermore, let the suppressing signal $\mathbf{c}$ be expressed as

$$\mathbf{c} = \mathbf{P}\mathbf{s} \ , \tag{2}$$

where $\mathbf{P} \in \mathbb{C}^{(N+L)\times L}$ and $\mathbf{s} \in \mathbb{C}^{L\times 1}$. The transmitted signal is then given as

$$\mathbf{t} = \mathbf{x} + \mathbf{c} = \mathbf{A}\mathbf{F}^{\mathrm{H}}\mathbf{M}\mathbf{d} + \mathbf{P}\mathbf{s} \ . \tag{3}$$

The design of both $\mathbf{s}$ and $\mathbf{P}$ will be discussed in detail in the following section; however for the time being, it suffices to say that $\mathbf{c} = \mathbf{P}\mathbf{s}$ will be designed to suppress both the spectral sidelobes and PAPR of the transmitted signal.

III. Suppressing Alignment

In this section, we introduce the concept of suppressing alignment and discuss its use in suppressing the spectral emissions of the transmitted OFDM signal. The application of suppressing alignment in reducing the PAPR will be discussed in the next section. Our main aim in this section is to construct the suppressing signal $\mathbf{c}$ in (3) so that the transmitted signal has better spectral emissions compared to conventional OFDM signals. More specifically, the suppressing signal $\mathbf{c}$ or equivalently $(\mathbf{P}\mathbf{s})$ is designed under two goals in mind: 1) to minimize the OOB power leakage of the transmitted signal in the adjacent band and 2) to avoid causing any interference to the information data carried by the OFDM symbol, in the sense that the receiver is able to recover all information data sent by the transmitter. In the subsequent discussion, the vector $\mathbf{s}$ will be designed to fulfill the first requirement while the matrix $\mathbf{P}$ is designed to satisfy the latter.

We first consider the construction of the matrix $\mathbf{P}$. Since the suppressing signal is added to the OFDM signal before transmission in (3), the information data carried by the OFDM signal is distorted and the receiver might not be able to recover the data if the suppressing signal is not properly designed. To achieve such proper design, we need to examine the received signal at the receiver after passing through the channel.

Let the channel between the transmitter and receiver be an i.i.d. Rayleigh fading channel represented by the vector $\mathbf{h} = [h_0, ..., h_l] \sim \mathcal{CN}(0, \mathbf{I}_{l+1}/(l+1))$. We can then express the received signal as

$$\mathbf{r} = \mathbf{H}\mathbf{t} + \mathbf{n} \ , \tag{4}$$

where $\mathbf{H} \in \mathbb{C}^{(N+L)(N+L)}$ is a Toeplitz matrix used to model the convolution between the transmitted signal $\mathbf{t}$ and the channel $\mathbf{h}$ and is given by

$$\mathbf{H} = \begin{bmatrix} h_0 & 0 & \cdots & 0 & h_l & \cdots & h_1 \\ \vdots & \ddots & \ddots & \ddots & \ddots & \ddots & \vdots \\ \vdots & \ddots & \ddots & \ddots & \ddots & \ddots & h_l \\ h_l & \cdots & \cdots & h_0 & 0 & \cdots & 0 \\ 0 & \ddots & \ddots & \ddots & \ddots & \ddots & \vdots \\ 0 & \ddots & 0 & h_l & \cdots & \cdots & h_0 \end{bmatrix} \ , \tag{5}$$

and $\mathbf{n} \in \mathbb{C}^{(N+L)\times 1} \sim \mathcal{CN}(0, \sigma^2\mathbf{I}_{N+L})$ is an additive white Gaussian noise (AWGN) vector. Assuming perfect synchronization and after the serial-to-parallel (S/P) conversion, the receiver removes the first L CP samples and then applies DFT. Using (3), the received signal after CP removal and DFT operation can be written as

$$\mathbf{y} = \mathbf{F}\mathbf{B}\mathbf{H}\mathbf{t} + \bar{\mathbf{n}} = \mathbf{F}\mathbf{B}\mathbf{H}\mathbf{A}\mathbf{F}^{\mathrm{H}}\mathbf{M}\mathbf{d} + \mathbf{F}\mathbf{B}\mathbf{H}\mathbf{P}\mathbf{s} + \bar{\mathbf{n}} \ , \tag{6}$$

where $\mathbf{B} \in \mathbb{R}^{N\times(N+L)}$ is the CP removal matrix and $\bar{\mathbf{n}} \in \mathbb{C}^{N\times 1}$ is a noise vector obtained after removing the first L samples from $\mathbf{n}$ and applying the DFT.

We are now ready to address the design of the matrix $\mathbf{P}$ by examining (6). As stated before, our goal in designing $\mathbf{P}$ is that the interference caused by the added suppressing signal should be zero at the receiver. Therefore, the following must hold true

$$\mathbf{F}\mathbf{B}\mathbf{H}\mathbf{P}\mathbf{s} = \mathbf{0} \ . \tag{7}$$

If (7) is satisfied, then, the received vector $\mathbf{y}$ in (6) becomes similar to legacy OFDM received data and the receiver would be able to apply single-tap equalization to recover the information symbols. Essentially, the information data in the vector $\mathbf{d}$ experiences zero interference from the suppressing signal.

Assuming perfect channel state information (CSI) at the transmitter, it is clear from (7) that if $\mathbf{P}$ belongs to the null-space of the matrix $\mathbf{B}\mathbf{H}$, i.e., $\ker(\mathbf{B}\mathbf{H})$, then (7) is satisfied regardless of the value of the vector $\mathbf{s}$. Using the rank-nullity theorem, the dimension of the null-space of $\mathbf{B}\mathbf{H} \in \mathbb{C}^{N\times(N+L)}$ is obtained as $\dim(\ker(\mathbf{B}\mathbf{H})) = N + L - \mathrm{rank}((\mathbf{B}\mathbf{H})) = L$, since $\mathrm{rank}(\mathbf{B}\mathbf{H}) = N$. Hence, by choosing $\mathbf{P}$ such that its columns span $\ker(\mathbf{B}\mathbf{H})$, the condition in (7) is satisfied and the receiver can recover the data using legacy OFDM reception. Accordingly, we design $\mathbf{P}$ such that

$$\mathrm{span}(\mathbf{P}) = \ker(\mathbf{B}\mathbf{H}) \ , \tag{8}$$

This article has been accepted for publication in a future issue of this journal, but has not been fully edited. Content may change prior to final publication. Citation information: DOI 10.1109/TCOMM.2015.2512603, IEEE Transactions on Communications

which is accomplished by choosing the columns of $\mathbf{P}$ as an orthogonal basis of $\ker(\mathbf{BH})$. Using the singular value decomposition, $\mathbf{BH}$ can be factored as

$$\mathbf{BH} = \mathbf{U}\mathbf{\Sigma}\mathbf{V}^{\mathrm{H}} \ , \tag{9}$$

where $\mathbf{U} \in \mathbb{C}^{N\times N}$, $\mathbf{\Sigma} \in \mathbb{C}^{N\times(N+L)}$ is a diagonal matrix holding the singular values of $\mathbf{BH}$, and $\mathbf{V} \in \mathbb{C}^{(N+L)\times(N+L)}$. If $\mathbf{V}$ is expressed as

$$\mathbf{V} = [\mathbf{v}_0 \ \mathbf{v}_1 \ \ldots \ \mathbf{v}_{N+L-1}] \ ,$$

then the last L columns of $\mathbf{V}$ constitute an orthogonal basis that spans the null-space of $(\mathbf{BH})$. Therefore, $\mathbf{P}$ is chosen as

$$\mathbf{P} = [\mathbf{v}_N \ \mathbf{v}_{N+1} \ \ldots \ \mathbf{v}_{N+L-1}] \ . \tag{10}$$

We remark that such construction of $\mathbf{P}$ allows interference-free transmission and is in principle similar to interference alignment (IA) [28]. In particular, $\mathbf{P}$ aligns the interference from the suppressing signal to the portion of the OFDM symbol spanned by the CP as shown in Fig. 1.

We now consider the design of the vector $\mathbf{s}$. Before we go into the details of our proposed method, let's first examine the interference caused by the transmitted signal (3) over the K subcarriers occupied by the user in the adjacent band. The signal spectrum of the transmitted signal (3) is given as

$$\boldsymbol{\mathcal{S}}_t = \mathbf{F}_{\zeta N,\beta}(\mathbf{A}\mathbf{F}^{\mathrm{H}}\mathbf{M}\mathbf{d} + \mathbf{P}\mathbf{s}) \ , \tag{11}$$

where ζ is the upsampling factor, i.e., ζ samples per subcarrier are considered, $\beta = N + L$, and $\mathbf{F}_{\zeta N,\beta}$ is an $\zeta N \times \beta$ DFT matrix. Using (11), the interference in the adjacent band can be given as

$$\boldsymbol{\mathcal{I}}_K = \boldsymbol{\mathcal{F}}_K(\mathbf{A}\mathbf{F}^{\mathrm{H}}\mathbf{M}\mathbf{d} + \mathbf{P}\mathbf{s}) = \underbrace{\boldsymbol{\mathcal{F}}_K\mathbf{A}\mathbf{F}^{\mathrm{H}}\mathbf{M}\mathbf{d}}_{\boldsymbol{\mathcal{F}}_{\mathbf{d}}} + \underbrace{\boldsymbol{\mathcal{F}}_K\mathbf{P}}_{\boldsymbol{\mathcal{F}}_{\mathbf{s}}}\mathbf{s} \ , \tag{12}$$

where $\boldsymbol{\mathcal{F}}_K$ is a sub-matrix of $\mathbf{F}_{\zeta N,\beta}$ containing only the rows that correspond to the subcarriers occupied by the adjacent user. The first term in (12) represents the OOB power leakage from the information data and the second term is the OOB power leakage from the suppressing signal $\mathbf{c}$. To minimize the interference power in the adjacent band, we calculate $\mathbf{s}$ such that

$$\mathbf{s} = \arg\min_{\mathbf{s}} \|\boldsymbol{\mathcal{F}}_{\mathbf{d}} + \boldsymbol{\mathcal{F}}_{\mathbf{s}}\mathbf{s}\|_2 \ \text{ subject to } \ \|\mathbf{s}\|_2^2 \leq \epsilon \ , \tag{13}$$

where ϵ is a power constraint on the vector $\mathbf{s}$ to avoid spending too much power on the suppressing signal. We note here that the power of the suppressing signal $\mathbf{c}$ is equal to the power of the vector $\mathbf{s}$ since $\mathbf{P}$ is an orthogonal matrix. The optimization problem in (13) is known as a least squares with a quadratic constraint (LSQI) problem. To solve this problem, we first consider the unconstrained least squares problem, i.e., without the power constraint. The solution to the least squares problem is

$$\mathbf{s} = -(\boldsymbol{\mathcal{F}}_{\mathbf{s}}{}^{\mathrm{H}}\boldsymbol{\mathcal{F}}_{\mathbf{s}})^{-1}\boldsymbol{\mathcal{F}}_{\boldsymbol{s}}{}^{\mathrm{H}}\boldsymbol{\mathcal{F}}_{\mathbf{d}} \ . \tag{14}$$

It is clear that the calculated $\mathbf{s}$ in (14) is also the solution to the problem in (13) if $\|\mathbf{s}\|_2^2 \leq \epsilon$, and in this case we have an analytical solution. However, if $\|\mathbf{s}\|_2^2 \geq \epsilon$, then there is no analytical solution and in order to solve the problem, we have to consider the following unconstrained problem

$$\mathbf{s} = \arg\min_{\mathbf{s}} \|\boldsymbol{\mathcal{F}}_{\mathbf{d}} + \boldsymbol{\mathcal{F}}_{\mathbf{s}}\mathbf{s}\|_2 + \lambda_0\|\mathbf{s}\|_2^2 \ , \tag{15}$$

where $\lambda_0 > 0$ is the Lagrange multiplier. The solution in this case is given by

$$\mathbf{s} = -(\boldsymbol{\mathcal{F}}_{\mathbf{s}}{}^{\mathrm{H}}\boldsymbol{\mathcal{F}}_{\mathbf{s}} + \lambda_0\mathbf{I})^{-1}\boldsymbol{\mathcal{F}}_{\mathbf{s}}{}^{\mathrm{H}}\boldsymbol{\mathcal{F}}_{\mathbf{d}} \ . \tag{16}$$

For a proper Lagrange multiplier, which can be found using the bi-section search algorithm [29], $\|\mathbf{s}\|_2^2 = \epsilon$. Alternatively, (13) can be solved numerically using any of the publicly available optimization solvers.

IV. Joint PAPR and OOB Power Leakage Reduction

PAPR is an important metric for multi-carrier systems. Any increase in the PAPR might drive the power amplifier at the transmitter to operate in the non-linear region. This can potentially cause spectral regrowth in the sidelobes, erasing any OOB reduction gains achieved before the power amplifier. Therefore, as an extension to the results in the previous section, we propose to jointly minimize the PAPR and OOB power leakage to avoid such problem.

The PAPR of the transmitted signal is the ratio of the maximum instantaneous power to the average power which is given as

$$\text{PAPR} = \frac{\|\mathbf{t}\|_\infty^2}{\frac{1}{(N+L)}\|\mathbf{t}\|_2^2} = \frac{\|\mathbf{x} + \mathbf{P}\mathbf{s}\|_\infty^2}{\frac{1}{(N+L)}\|\mathbf{x} + \mathbf{P}\mathbf{s}\|_2^2} \ . \tag{17}$$

Accordingly, to minimize the OOB interference as well as the PAPR, we extend the optimization problem in (13) as follows

$$\begin{aligned} &\mathbf{s} = \arg\min_{\mathbf{s}} (1-\lambda)\|\boldsymbol{\mathcal{F}}_{\mathbf{d}} + \boldsymbol{\mathcal{F}}_{\mathbf{s}}\mathbf{s}\|_2 + \lambda\|\mathbf{x} + \mathbf{P}\mathbf{s}\|_\infty \ , \\ &\text{subject to } \ \|\mathbf{s}\|_2^2 \leq \epsilon \ , \end{aligned} \tag{18}$$

where the weighting factor, $\lambda \in [0, 1]$, is for controlling the amount of minimization for both OOB power leakage and PAPR. This adaptation parameter can be adjusted to emphasize one problem over the other depending on the system design requirements. For example, when $\lambda = 0$, the objective function turns into a pure OOB power leakage reduction problem and (18) is equivalent to (13). On the other hand, (18) is a pure PAPR reduction problem when $\lambda = 1$. Similar to (13), the amount of power consumed by the suppressing signal is controlled by ϵ.

Both the objective function and the constraint in (18) are convex which renders the problem as a convex optimization problem that can be solved numerically by any convex optimization solver. In this work, we utilize YALMIP [30], a free optimization package that is easily integrated with MATLAB, and MOSEK [31] as the underlying solver to obtain a numerical solution to (18).

V. Practical Implementation Issues

A. Imperfect channel estimation

In practice, the assumption of perfect channel knowledge at the transmitter might not be valid. In this subsection, we analyze the performance of the proposed algorithm when the

This article has been accepted for publication in a future issue of this journal, but has not been fully edited. Content may change prior to final publication. Citation information: DOI 10.1109/TCOMM.2015.2512603, IEEE Transactions on Communications

transmitter has imperfect CSI. The channel is estimated at the receiver and the CSI is fed back to the transmitter. The transmitter then uses this CSI to generate the suppressing signal $\mathbf{c} = \mathbf{P}\mathbf{s}$. To evaluate the impact of channel estimation errors, we assume that the channel known at the transmitter is different than the actual channel that the signal is transmitted through. We model the noisy channel estimation as

$$\hat{\mathbf{H}} = \mathbf{H} + \mathbf{E} \ , \tag{19}$$

where $\mathbf{E} = \sigma_e \mathbf{\Omega}$ is the channel error matrix and $\mathbf{\Omega}$ is Toeplitz with the same structure as (5). The non-zero entries of $\mathbf{\Omega}$ are i.i.d. complex Gaussian with zero mean and unit variance. We quantify the error in channel estimation by the mean square error (MSE) σ_e^2 defined as [32]

$$\sigma_e^2 = \frac{\mathbb{E}[|\hat{h_{ij}} - h_{ij}|^2]}{\mathbb{E}[|h_{ij}|^2]} \ . \tag{20}$$

The received signal after CP removal and DFT operation is given by (6), where the precoding matrix $\mathbf{P}$ is designed based on knowledge of the channel at the transmitter. If the channel $\mathbf{H}$ communicated back to the transmitter by the receiver is erroneous, then $\mathbf{P}$ is designed based on $\mathbf{H}$ as opposed to the true channel $\hat{\mathbf{H}}$. Therefore, the second term in (6) would not vanish, i.e., (7) is not true any more. This effectively means that the suppressing signal leaks into the data part of the OFDM symbol instead of precisely being aligned with the CP duration. Nevertheless, the erroneous channel information does not effect the OOB power leakage and PAPR reduction performance of the proposed method, since the suppressing signal is still designed based on (13) or (18).

The average power leakage of the suppressing signal into the data part of the received OFDM symbol can be expressed as

$$\xi = \frac{1}{N}\mathbb{E}[\|\mathbf{B}\hat{\mathbf{H}}\mathbf{P}\mathbf{s}\|_2^2] \ . \tag{21}$$

To evaluate the above the expression, we utilize the closed-form expression for $\mathbf{s}$ in (16), which after substituting $\boldsymbol{\mathcal{F}}_{\mathbf{d}}$ from (12), can be written as

$$\mathbf{s} = \underbrace{-(\boldsymbol{\mathcal{F}}_{\mathbf{s}}{}^{\mathrm{H}}\boldsymbol{\mathcal{F}}_{\mathbf{s}} + \lambda_0\mathbf{I})^{-1}\boldsymbol{\mathcal{F}}_{\mathbf{s}}{}^{\mathrm{H}}\boldsymbol{\mathcal{F}}_K\mathbf{A}\mathbf{F}^{\mathrm{H}}\mathbf{M}}_{\mathbf{\Phi}}\mathbf{d} = \mathbf{\Phi}\mathbf{d} \ . \tag{22}$$

Substituting $\hat{\mathbf{H}}$ from (19) and the above expression for $\mathbf{s}$, the mean leaked power in (21) can now be evaluated as

$$\begin{aligned}\xi &= \frac{1}{N}\mathbb{E}\big[\mathrm{tr}[(\mathbf{B}(\mathbf{H}+\mathbf{E})\mathbf{P}\mathbf{\Phi}\mathbf{d})^{\mathrm{H}}(\mathbf{B}(\mathbf{H}+\mathbf{E})\mathbf{P}\mathbf{\Phi}\mathbf{d})]\big] \\ &= \frac{1}{N}\mathbb{E}\big[\mathrm{tr}[\mathbf{d}^{\mathrm{H}}\mathbf{\Phi}^{\mathrm{H}}\mathbf{P}^{\mathrm{H}}(\mathbf{H}+\mathbf{E})^{\mathrm{H}}\mathbf{B}^{\mathrm{H}}\mathbf{B}(\mathbf{H}+\mathbf{E})\mathbf{P}\mathbf{\Phi}\mathbf{d}]\big] \\ &= \frac{1}{N}\mathrm{tr}\big[\mathbf{\Phi}^{\mathrm{H}}\mathbf{P}^{\mathrm{H}}\mathbb{E}[(\mathbf{H}+\mathbf{E})^{\mathrm{H}}\mathbf{B}^{\mathrm{H}}\mathbf{B}(\mathbf{H}+\mathbf{E})]\mathbf{P}\mathbf{\Phi}\mathbb{E}[\mathbf{d}\mathbf{d}^{\mathrm{H}}]\big]\end{aligned}$$

Since $\mathbf{BHP} = \mathbf{0}$ and the data vector $\mathbf{d}$ is assumed to have zero mean and covariance $\mathbb{E}[\mathbf{d}\mathbf{d}^{\mathrm{H}}] = \mathbf{I}_{N_d}$, we arrive at

$$\xi = \frac{1}{N}\mathrm{tr}\big[\mathbf{\Phi}^{\mathrm{H}}\mathbf{P}^{\mathrm{H}}\mathbb{E}[\mathbf{E}^{\mathrm{H}}\mathbf{B}^{\mathrm{H}}\mathbf{B}\mathbf{E}]\mathbf{P}\mathbf{\Phi}\big] \tag{23}$$

$$= \frac{1}{N}\mathrm{tr}\big[\mathbb{E}[\mathbf{E}\mathbf{P}\mathbf{\Phi}\mathbf{\Phi}^{\mathrm{H}}\mathbf{P}^{\mathrm{H}}\mathbf{E}^{\mathrm{H}}]\mathbf{B}^{\mathrm{H}}\mathbf{B}\big] \ . \tag{24}$$

Let $\mathbf{Z} = \mathbf{P}\mathbf{\Phi}\mathbf{\Phi}^{\mathrm{H}}\mathbf{P}^{\mathrm{H}}$, $\mathbf{Y} = \mathbf{E}\mathbf{Z}\mathbf{E}^{\mathrm{H}}$ and the projection matrix $\mathbf{G} = \mathbf{B}^{\mathrm{H}}\mathbf{B}$ defined as

$$\mathbf{G} = \begin{bmatrix} \mathbf{0}_{L\times L} & \mathbf{0}_{L\times N} \\ \mathbf{0}_{N\times L} & \mathbf{I}_{N\times N} \end{bmatrix} \ .$$

Thus,

$$\xi = \frac{1}{N}\mathrm{tr}\big[\mathbb{E}[\mathbf{Y}]\mathbf{G}\big] \ . \tag{25}$$

Using the definition for $\mathbf{Y}$ above as well as the Toeplitz property of the error matrix i.e., $E_{ij} = e_{i-j}$, the expectation in (25) can now be evaluated as

$$\mathbb{E}[Y]_{ij} = \sum_{kl}\mathbb{E}[E_{ik}Z_{kl}E_{jl}^*] = \sum_{kl}\mathbb{E}[e_{i-k}Z_{kl}e_{j-l}^*] \ , \tag{26}$$

and since $\mathbb{E}[e_i e_j^*] = \frac{1}{L}\sigma_e^2\delta'_{ij}$, we then have

$$\mathbb{E}[Y_{ij}] = \frac{1}{L}\sigma_e^2\sum_{kl}Z_{kl}\delta'_{i-k,j-l} \ . \tag{27}$$

Due to the structure of the projection matrix $\mathbf{G}$, it only selects entries with $i = j = L+1, L+2, ..., L+N$. Accordingly, we arrive at the final expression for the leaked power as

$$\xi = \frac{1}{N}\mathrm{tr}\big[\mathbb{E}[\mathbf{Y}]\mathbf{G}\big] = \frac{1}{LN}\sigma_e^2\sum_{i=L+1}^{N+L}\sum_{k,l=1}^{N+L}Z_{kl}\delta'_{i-k,i-l} \tag{28}$$

$$= \frac{1}{LN}\sigma_e^2\sum_{k=1}^{N+L}Z_{kk}\Psi_k \ , \tag{29}$$

where $\Psi_k = \sum_{i=L+1}^{N+L}\delta'_{i-k,i-k}$ and is equal to

$$\Psi_k = \begin{cases} k-1 \ , & 1 \le k \le L \\ L \ , & L+1 \le k \le N+1 \\ N+L-k+1 \ , & N+2 \le k \le N+M \\ 0 \ , & \text{otherwise} \end{cases} \ . \tag{30}$$

It is worth noting that the closed form expression in (29) represents the power leakage when we consider only the OOB reduction but not the joint reduction of PAPR and OOB since a closed-form solution for the suppressing signal does not exist in the latter case. Alternatively, the power leakage in the case of joint reduction of OOB and PAPR is evaluated through simulation.

B. Synchronization

Another important factor for proper operation of the proposed method is time synchronization. It is very critical to know the start of the transmitted frame in order to guarantee exact alignment of the suppressing signal and zero interference to the information symbols. Synchronization in OFDM systems is usually achieved by either transmitting a known training sequence (preamble) [33] or by exploiting the redundancy of the CP [34], [35]. Preamble based synchronization algorithms can be incorporated easily with our proposed approach, where the suppressing signal is not generated during the synchronization phase. However, this absence of the suppressing signal during the synchronization phase will not have any detrimental effects on the OOB

This article has been accepted for publication in a future issue of this journal, but has not been fully edited. Content may change prior to final publication. Citation information: DOI 10.1109/TCOMM.2015.2512603, IEEE Transactions on Communications

interference or PAPR since the preamble is usually made up of pseudo-random (PN) sequences that have low OOB leakage and PAPR [36].

CP-based synchronization is based on the fact that the CP samples are similar to the corresponding data samples at the end of the OFDM symbol. These similar samples in the CP and the data portion of the OFDM symbol are spaced by N samples apart. Using a sliding window correlator, this information can be used to detect the start of the OFDM symbol. However, after applying the suppressing signal to the OFDM signal, the CP samples are no longer a cyclic extension of the OFDM symbol. As such, the CP may no longer be utilized for synchronization purposes. To overcome this issue the suppressing signal can be designed so that it leaves part of the CP and the corresponding samples in the data duration of the OFDM symbol unaffected. Accordingly, part of the CP samples are used by the suppressing signal for OOB and PAPR reduction while the rest are used for synchronization. This partial CP usage is only during the synchronization phase, once synchronization is established the full CP length can be utilized by the suppressing signal.

Let R denote the number of CP samples used for synchronization located at the start of the OFDM symbol. As mentioned above, the R CP samples as well as the corresponding R data samples are not distorted in any way by the suppressing signal. As such, the transmitted signal during the synchronization period will be different than the one in (3). We introduce the matrix $\mathbf{W}$ to preserve the CP samples and their corresponding data samples as follows

$$\mathbf{t}_{\mathrm{s}} = \mathbf{x} + \mathbf{c}_{\mathrm{s}} = \mathbf{A}\mathbf{F}^{\mathrm{H}}\mathbf{M}\mathbf{d} + \mathbf{W}\mathbf{P}\mathbf{s}_{\mathrm{s}} \ , \tag{31}$$

where $\mathbf{W} \in \mathbb{R}^{(N+L)\times(N+L-2R)}$ and is constructed by selecting the $N+L-2R$ columns of $\mathbf{I}_{(N+L)}$ corresponding to the samples being protected from any distortion caused by the suppressing signal. Similar to (8), the alignment matrix $\mathbf{P}$ is designed such that $\mathrm{span}(\mathbf{P}) = \ker(\mathbf{BHW})$. The only difference now is that $\mathrm{rank}((\mathbf{BHW})) = N$, and accordingly $\dim(\ker(\mathbf{BHW})) = (N+L-2R) - \mathrm{rank}((\mathbf{BHW})) = L-2R$. Therefore, $R < \frac{L}{2}$ for $\ker(\mathbf{BHW})$ to exist. This practically means that the partial CP samples cannot be larger than half of the full CP length. Furthermore, compared to using the full L CP samples, the degrees of freedom utilized by the vector $\mathbf{s}_{\mathrm{s}}$ to suppress the spectrum and PAPR of the transmitted signal in (31) are reduced to $L-2R$ during the synchronization phase. As such, this results in some degradation in the PAPR and OOB reduction performance. However, this performance loss is only during the synchronization phase and once synchronization has been established, performance will fall back to that of the full CP.

VI. Numerical Results

In this section, we evaluate the OOB reduction as well as the PAPR performance of the proposed method with computer simulations. For simulation tractability, we consider an OFDM system with $N = 64$ subcarriers and a CP length of $L = 16$ samples. Additionally, we assume that the OFDM transmitter detects an adjacent user spanning 10 subcarriers within its band of transmission. Thus, these subcarriers are disabled by the OFDM system, while the remaining subcarriers are utilized for transmission. The transmission is carried through a multipath Rayleigh fading channel with $L+1$ taps and a uniform power delay profile (PDP). To illustrate the OOB power leakage reduction performance of the proposed method, 10^4 4QAM symbols are generated randomly and the Welch's averaged periodogram method is then used to estimate the power spectrum. We evaluate the the PAPR reduction performance using the complimentary cumulative distribution function (CCDF). Furthermore, in all simulations, we constrain the power of the suppressing signal to be a fraction of the power of the plain OFDM signal, i.e., $\epsilon = \alpha\|\mathbf{x}\|_2^2$, where α is a parameter that controls the power allocated to the suppressing signal. The maximum power percentage consumed by the suppressing signal is $\frac{\alpha}{1+\alpha}$ of the total available power budget. In all simulations, we assume the total power budget is shared between the OFDM signal and the suppressing signal.

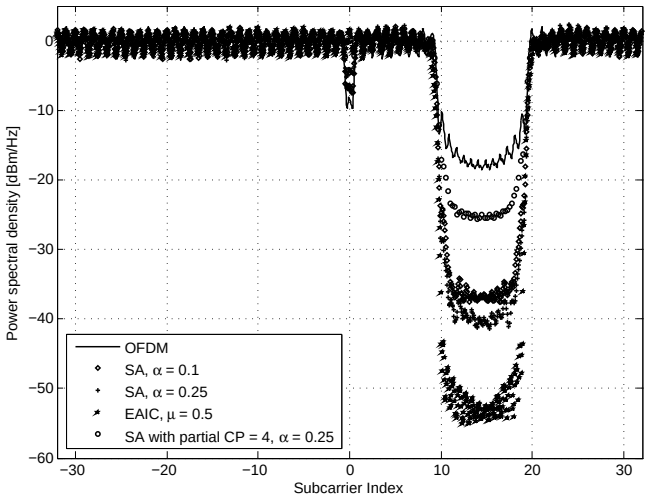

Fig. 2: Power spectral density for 4-QAM, $\lambda = 0$.

A. PAPR and OOB power leakage reduction performance

First, we evaluate the OOB power leakage reduction of the proposed method based on (13), without considering the PAPR reduction, i.e., $\lambda = 0$. As shown in Fig. 2, the proposed method achieves remarkable levels of OOB power leakage reduction compared to plain OFDM. We also note that the amount of OOB power leakage reduction increases as α increases, i.e., as more power is allocated to the suppressing signal. For example, for $\alpha = 0.1$ or approximately $\%9$ of the total power budget, the suppressing signal reduces the OOB leakage by roughly 18 dB, while approximately 22 dB reduction is obtained when $\alpha = 0.25$ or $\%20$ of the total power budget. We also note that the performance depends on the number of CP samples used by the suppressing signal as demonstrated by the case of partial CP usage in Fig. 2, where approximately 7 dB reduction compared to OFDM is achieved using only 4 CP samples. We note here that partial CP is used only during the synchronization phase. By examining Fig. 2, we observe a slight overshoot in the spectrum close to the band edges,

This article has been accepted for publication in a future issue of this journal, but has not been fully edited. Content may change prior to final publication. Citation information: DOI 10.1109/TCOMM.2015.2512603, IEEE Transactions on Communications

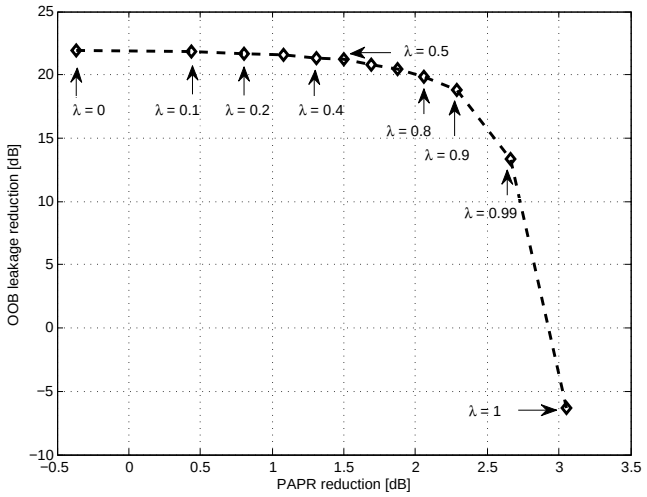

Fig. 3: Performance trade-off between OOB reduction and PAPR reduction when $\alpha = 0.25$.

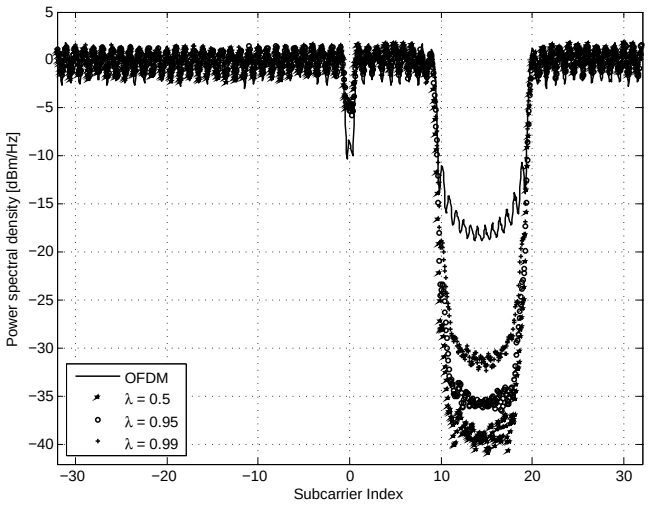

Fig. 4: Power spectral density for 4-QAM for $\alpha = 0.25$.

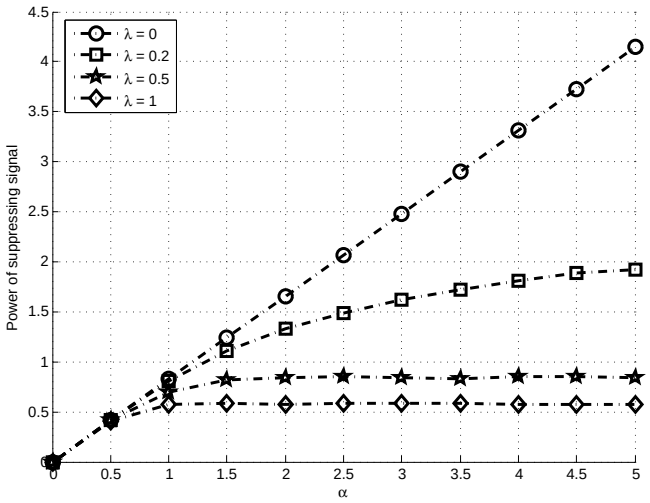

Fig. 5: Power of suppressing signal for different values of λ.

especially as α grows. This can be attributed to the fact that the suppressing signal puts more power on the subcarriers close to the edges because of their high contribution to the OOB power leakage. In Fig. 2, we also show the performance of the extended active interference cancellation (EAIC) scheme in [11] evaluated under the same spectral efficiency as our proposed approach. Although the EAIC scheme achieves better OOB reduction compared to our proposed method, it does so by introducing distortion on the data subcarriers which leads to degradation in the BER performance as will be shown below.

Fig. 3 shows the trade-off between the PAPR reduction and OOB reduction performance for the joint optimization problem in (18). The trade-off is visualized by showing the average reduction in both OOB leakage and PAPR as a function of the adaptation parameter λ when α is set to 0.25. We note that when $\lambda = 0$, the optimization problem (18) is equivalent to (13), where only the OOB interference is minimized. The average reduction in OOB interference in this case is approximately 22 dB, which agrees with the results in Fig. 2 when $\alpha = 0.25$. Increasing λ beyond zero, reduces the gain in terms of OOB leakage reduction while gradually improving the PAPR reduction performance. As shown in Fig. 3, a maximum average PAPR reduction of more than 3 dB is obtained when $\lambda = 1$. However, in this case, and as expected, there is no gain in the OOB interference reduction. In fact, the OOB power leakage increases due to the fact that the suppressing signal places some power in the adjacent band. The same is true when $\lambda = 0$, where a pure OOB leakage reduction leads to a slight increase in the PAPR as shown in Fig. 3. The OOB power leakage reduction for different values of λ is shown in Fig. 4. Here, the power of the suppressing signal is fixed at 20% of the total power budget, i.e., $\alpha = 0.25$. These results in Fig. 4 expand over the mean OOB reduction results in Fig. 3 by showing the actual power spectral density of the transmitted signal. As seen from Fig. 4, the OOB leakage is significantly reduced as λ decreases, which is rather expected as more emphasis is put on the OOB leakage reduction relative to the PAPR reduction. In order to understand the behavior of the joint optimization problem in (18) with regard to the actual power allocated to the suppressing signal, we plot the average power of the suppressing signal against α for different values of the adaptation parameter λ, as shown in Fig. 5. The results in Fig. 5 indicate that when PAPR is not considered, i.e., $\lambda = 0$, the actual power used by the suppressing signal changes linearly with α. In other words, all the power allocated to the suppressing signal will be completely utilized to reduce the spectral sidelobes. However, as the PAPR reduction is slowly factored into the problem, the utilization of the allocated power decreases. Specifically, we observe that as the adaptation parameter λ increases gradually, the suppressing signal uses less power to jointly reduce both PAPR and spectral leakage. For the extreme case of $\lambda = 1$, i.e., when it is a pure PAPR reduction problem, the power of the suppressing signal completely saturates regardless of how much power is allocated through the parameter α.

We now turn to characterizing the performance of the proposed method with regard to PAPR reduction. In order to do

This article has been accepted for publication in a future issue of this journal, but has not been fully edited. Content may change prior to final publication. Citation information: DOI 10.1109/TCOMM.2015.2512603, IEEE Transactions on Communications

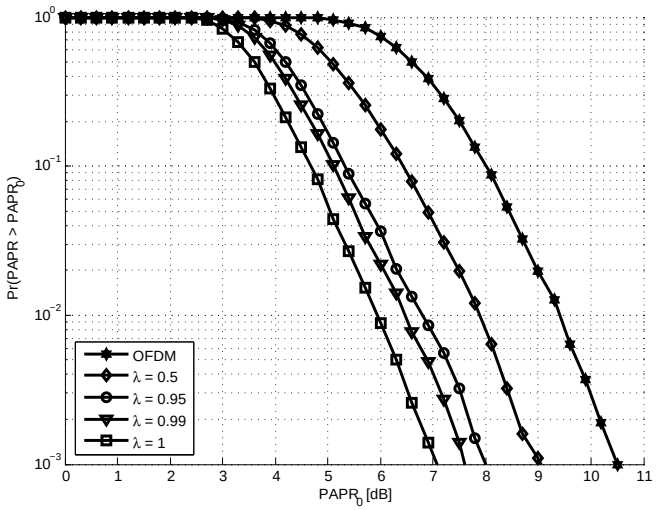

Fig. 6: PAPR performance for 4-QAM when $\alpha = 0.25$.

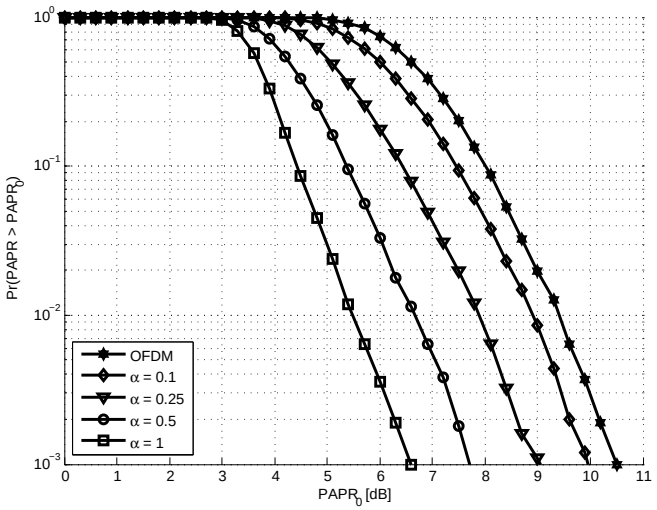

Fig. 7: PAPR performance for 4-QAM when $\lambda = 0.5$.

that, we consider the actual instantaneous power distribution of the transmitted signal and plot its CCDF as shown in Fig. 6 and Fig. 7. In Fig. 6, we show the PAPR performance for different values of λ and a fixed $\alpha = 0.25$. We start by noting that remarkable reduction in the PAPR is obtained as shown in Fig. 6. In particular, this reduction increases as the adaptation parameter λ grows, i.e., the PAPR reduction is emphasized compared to the power leakage reduction. For example, in the extreme case of $\lambda = 1$, the PAPR of the transmitted signal is around 7 dB at a probability of 10^{-3}; a reduction of approximately 3.5 dB from that of the plain OFDM signal. However, there is no reduction in the OOB interference when $\lambda = 1$. Nonetheless, decent improvements in the PAPR performance can still be obtained even for small values of λ while simultaneously allowing large reductions in the OOB interference. For example, when λ is set to 0.5, the PAPR of the transmitted signal is around 9 dB compared to 10.5 dB at a probability of 10^{-3} for plain OFDM. At the same value of λ, the OOB power of the transmitted signal is around -39 dB compared to -18 dB for plain OFDM; a 21 dB reduction as shown in Fig. 4. The variation of the PAPR performance with the suppressing signal power is shown in Fig. 7. In the extreme case of having a suppressing signal consuming $\%50$ as the total power budget, i.e., when $\alpha = 1$, the PAPR is reduced by 4 dB at a probability of 10^{-3}. Alternatively, for $\alpha = 0.25$, the PAPR is reduced by approximately 1.5 dB, showing that a slight increase in the power allocated to the suppressing signal can still lead to good PAPR reduction.

B. Bit error performance

The BER performance of the proposed method as well as the EAIC scheme [11] for 16QAM and 64QAM is shown in Fig. 8. The performance is evaluated in a Rayleigh multipath fading channel. The EAIC clearly has an error floor due the distortion it introduces to the data subcarriers. On the contrary, our proposed appraoch offers a distortion-free transmission without any changes to the receiver structure. It's worth noting here that the small offset in performance between the proposed scheme and plain OFDM is due to the fact that the total power budget is shared between the suppressing signal and the OFDM signal.

The BER results in Fig. 8 are obtained with the assumption that there is no channel estimation errors. However, and as mentioned before if the correct channel is not perfectly known at the transmitter, the suppressing signal will leak into the OFDM signal. In Fig. 9, we show the analytical leaked power expression in (29) as well the simulated leaked power plotted against the MSE of different channel errors when we consider the OOB interference reduction only, i.e., $\lambda = 0$. It is clear that the leaked power values obtained from the closed-form expression in (29) match those obtained from the simulation. The leaked power when we jointly consider the OOB and PAPR reduction is shown in Fig. 10, where the results are obtained through simulation since there is no closed-form expression for the leaked power in this case.

To assess the impact of the power leakage due to the channel estimation errors on the BER performance, we conducted Monte Carlo simulations of the proposed algorithm for different values of the signal-to-noise ratio (SNR) as shown in Fig. 11. Our simulations are bench-marked against the error performance of plain OFDM under the same noisy channel estimation. Other than a small offset as observed in Fig. 11 which is due the total power budget being shared, the error performance of the suppressing alignment algorithm is identical to that of standard OFDM under channel estimation errors. This can be explained by looking at Fig. 10. There, the average power leakage of the suppressing signal into the data part of the received OFDM symbol defined in (21) is plotted against the MSE of the channel for different values of α. In Fig. 10, the leaked power is at least 8 dB less than the channel MSE when $\alpha = 0.25$. Essentially, the noisy channel dominates the error performance. As such, no degradation in the BER is observed as shown in Fig. 11 when $\alpha = 0.25$.

This article has been accepted for publication in a future issue of this journal, but has not been fully edited. Content may change prior to final publication. Citation information: DOI 10.1109/TCOMM.2015.2512603, IEEE Transactions on Communications

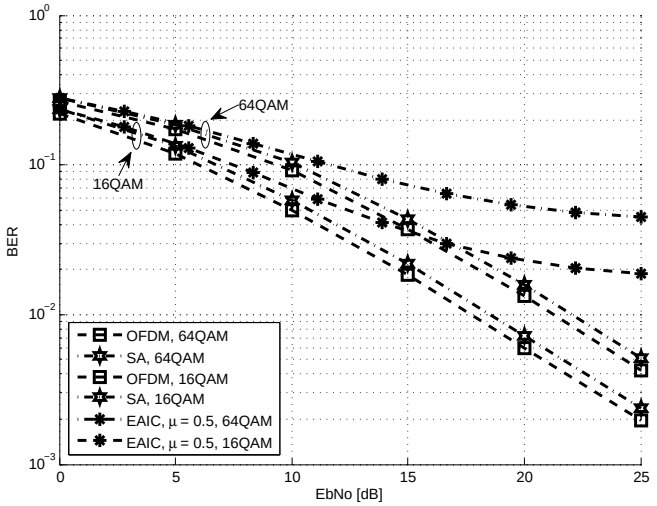

Fig. 8: BER performance under Rayleigh multipath fading channels, $\lambda = 0.5,\ \alpha = 0.25$.

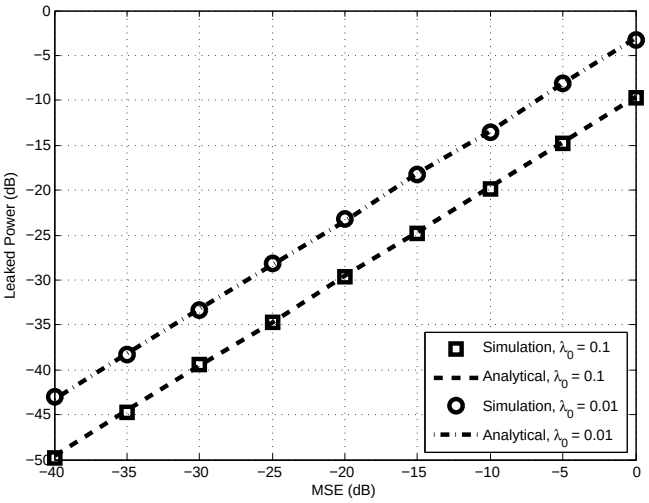

Fig. 9: Leaked power in (29) under imperfect CSI, $\lambda = 0$.

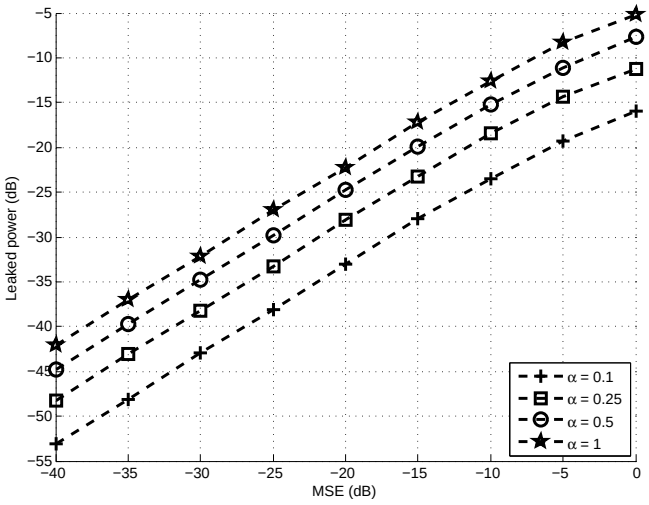

Fig. 10: Leaked power of the suppressing signal under imperfect CSI, $\lambda = 0.5$.

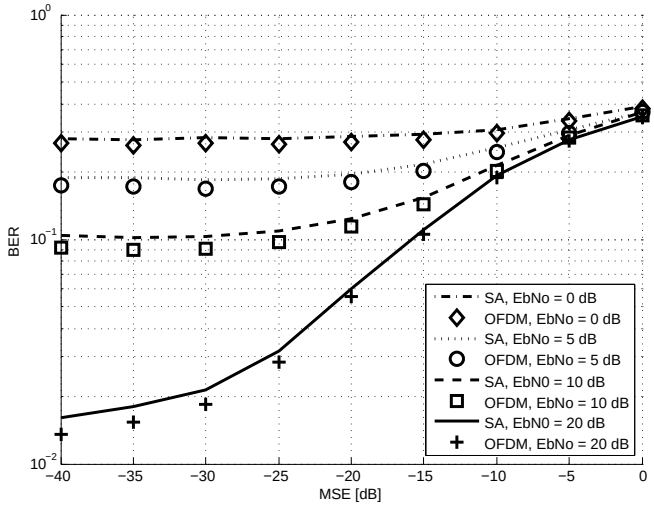

Fig. 11: BER performance for 64-QAM under imperfect CSI, $\lambda = 0.5,\ \alpha = 0.25$.

VII. Conclusion

In this work, we have proposed an approach called *suppressing alignment* that generates a suppressing signal to jointly reduce the OOB power leakage and PAPR of OFDM-based systems. The main advantage of the proposed method is that it does not reduce the spectral efficiency as it exploits the inherent redundancy in OFDM provided by the CP. We have also shown that the suppressing signal can be constructed in such a way that it does not create any interference to the information data carried in the OFDM symbol. In particular, by utilizing the wireless channel, the suppressing signal is aligned with the CP duration at the receiver, effectively creating an interference-free transmission with a BER performance similar to legacy OFDM without requiring any change in the receiver structure. The effectiveness of the proposed approach in obtaining remarkable reduction in both the OOB power leakage and PAPR is shown through computer simulations. We showed the performance trade-off between the OOB power leakage reduction and PAPR reduction where both can flexibly be controlled through an adaptation parameter. Furthermore, we investigated the impact of imperfect CSI on the error performance of the proposed approach. Simulation results show no degradation in the BER performance of the proposed approach compared to legacy OFDM under the same noisy channel errors.

References

[1] D. Qu, J. Ding, T. Jiang, and X. Sun, "Detection of non-contiguous OFDM symbols for cognitive radio systems without out-of-band spectrum synchronization," *IEEE Trans. Wireless Commun.*, vol. 10, no. 2, pp. 693–701, February. 2011.

[2] A. Şahin, I. Güvenç, and H. Arslan, "A survey on multicarrier communications: Prototype filters, lattice structures, and implementation aspects," *IEEE Commun. Surveys Tuts.*, vol. 16, no. 3, pp. 1312–1338, Third Quarter 2014.

[3] T. Jiang and Y. Wu, "An overview: Peak-to-average power ratio reduction techniques for OFDM signals," *IEEE Trans. Broadcasting.*, vol. 54, no. 2, pp. 257–268, June. 2008.

[4] E. Costa, M. Midrio, and S. Pupolin, "Impact of amplifier nonlinearities on OFDM transmission system performance," *IEEE Commun. Lett.*, vol. 3, no. 2, pp. 37–39, February. 1999.

[5] T. Weiss, J. Hillenbrand, A. Krohn, and F. Jondral, "Mutual interference in OFDM-based spectrum pooling systems," in *Proc. IEEE Vehic. Technol. Conf. (VTC)*, vol. 4, May 2004, pp. 1873–1877.

[6] A. Sahin and H. Arslan, "Edge windowing for OFDM based systems," *IEEE Commun. Lett.*, vol. 15, no. 11, pp. 1208–1211, Nov. 2011.

[7] H. Mahmoud and H. Arslan, "Sidelobe suppression in OFDM-based spectrum sharing systems using adaptive symbol transition," *IEEE Commun. Lett.*, vol. 12, no. 2, pp. 133–135, Feb. 2008.

[8] H. Yamaguchi, "Active interference cancellation technique for MB-OFDM cognitive radio," in *Proc. IEEE European Microwave Conference*, vol. 2, 2004, pp. 1105–1108.

[9] S. Brandes, I. Cosovic, and M. Schnell, "Reduction of out-of-band radiation in OFDM systems by insertion of cancellation carriers," *IEEE Commun. Lett.*, vol. 10, no. 6, pp. 420–422, Jun. 2006.

[10] ——, "Sidelobe suppression in OFDM systems by insertion of cancellation carriers," in *Proc. IEEE Vehic. Technol. Conf. (VTC)*, vol. 1, 2005, pp. 152–156.

[11] D. Qu, Z. Wang, and T. Jiang, "Extended active interference cancellation for sidelobe suppression in cognitive radio OFDM systems with cyclic prefix," *IEEE Trans. Vehicular. Technol.*, vol. 59, no. 4, pp. 1689–1695, May. 2010.

[12] I. Cosovic, S. Brandes, and M. Schnell, "Subcarrier weighting: a method for sidelobe suppression in OFDM systems," *IEEE Commun. Lett.*, vol. 10, no. 6, pp. 444–446, Jun. 2006.

[13] J. van de Beek, "Sculpting the multicarrier spectrum: a novel projection precoder," *IEEE Commun. Lett.*, vol. 13, no. 12, pp. 881–883, Dec. 2009.

[14] A. Tom, A. Sahin, and H. Arslan, "Mask compliant precoder for OFDM spectrum shaping," *IEEE Commun. Lett.*, vol. 17, no. 3, pp. 447–450, Mar. 2013.

[15] J. van de Beek, "Orthogonal multiplexing in a subspace of frequency well-localized signals," *IEEE Commun. Lett.*, vol. 14, no. 10, pp. 882–884, Oct. 2010.

[16] M. Ma, X. Huang, B. Jiao, and Y. Guo, "Optimal orthogonal precoding for power leakage suppression in DFT-based systems," *IEEE Trans. Commun.*, vol. 59, no. 3, pp. 844–853, Mar. 2011.

[17] C.-D. Chung, "Spectrally precoded OFDM," *IEEE Trans. Commun.*, vol. 54, no. 12, pp. 2173–2185, Dec. 2006.

[18] J. Van De Beek and F. Berggren, "N-continuous OFDM," *IEEE Commun. Lett.*, vol. 13, no. 1, pp. 1–3, Jan. 2009.

[19] Y. Zheng, J. Zhong, M. Zhao, and Y. Cai, "A precoding scheme for N-continuous OFDM," *IEEE Commun. Lett.*, vol. 16, no. 12, pp. 1937–1940, Dec. 2012.

[20] S. H. Han and J. H. Lee, "An overview of peak-to-average power ratio reduction techniques for multicarrier transmission," *IEEE Trans. Wireless Commun.*, vol. 12, no. 2, pp. 56–65, April. 2005.

[21] A. Ghassemi, L. Lampe, A. Attar, and T. Gulliver, "Joint sidelobe and peak power reduction in ofdm-based cognitive radio," in *IEEE Veh. Technol. Conf. (VTC)*, Sept. 2010, pp. 1–5.

[22] M. Senst, M. Jordan, M. Dorpinghaus, M. Farber, G. Ascheid, and H. Meyr, "Joint reduction of peak-to-average power ratio and out-of-band power in OFDM systems," in *Proc. IEEE Global Telecommun. Conf. (GLOBECOM)*, 2007, pp. 3812–3816.

[23] E. Guvenkaya, A. Tom, and H. Arslan, "Joint sidelobe suppression and papr reduction in OFDM using partial transmit sequences," in *Military Communications Conference, MILCOM 2013 - 2013 IEEE*, Nov. 2013, pp. 95–100.

[24] C. Ni, T. Jiang, and W. Peng, "Joint papr reduction and sidelobe suppression using signal cancellation in NC-OFDM based cognitive radio systems," *IEEE Trans. Vehicular Technol*, vol. PP, no. 99, pp. 1–1, 2014.

[25] M. Maso, M. Debbah, and L. Vangelista, "A distributed approach to interference alignment in OFDM-based two-tiered networks," *IEEE Trans. Vehicular Technol.*, vol. 62, no. 5, pp. 1935–1949, Jun. 2013.

[26] H. Qin, Y. Sun, T.-H. Chang, X. Chen, C.-Y. Chi, M. Zhao, and J. Wang, "Power allocation and time-domain artificial noise design for wiretap OFDM with discrete inputs," *IEEE Trans. Wireless Commun.*, vol. 12, no. 6, pp. 2717–2729, Jun. 2013.

[27] M. Maso, S. Lakshminarayana, T. Quek, and H. Poor, "A composite approach to self-sustainable transmissions: Rethinking OFDM," *IEEE Trans. Commun.*, vol. PP, no. 99, pp. 1–1, 2014.

[28] V. Cadambe and S. Jafar, "Interference alignment and degrees of freedom of the k-user interference channel," *IEEE Trans. Information Theory.*, vol. 54, no. 8, pp. 3425–3441, Aug. 2008.

[29] S. Boyd and L. Vandenberghe, *Convex Optimization*. New York, NY, USA: Cambridge University Press, 2004.

[30] J. Löfberg, "YALMIP : a toolbox for modeling and optimization in MATLAB," in *Proc. IEEE International Symposium on Computer Aided Control Systems Design (CACSD)*, Sep. 2004, pp. 284–289.

[31] MOSEK. [Online]. Available: http://www.mosek.com

[32] C. Wang, E. Au, R. Murch, W. H. Mow, R. Cheng, and V. Lau, "On the performance of the MIMO zero-forcing receiver in the presence of channel estimation error," *IEEE Trans. Wireless Commun.*, vol. 6, no. 3, pp. 805–810, March 2007.

[33] T. Schmidl and D. Cox, "Robust frequency and timing synchronization for OFDM," *IEEE Trans. Commun.*, vol. 45, no. 12, pp. 1613–1621, Dec 1997.

[34] S. Ma, X. Pan, G.-H. Yang, and T.-S. Ng, "Blind symbol synchronization based on cyclic prefix for OFDM systems," *IEEE Trans. Vehicular Technol.*, vol. 58, no. 4, pp. 1746–1751, May 2009.

[35] J.-J. van de Beek, M. Sandell, M. Isaksson, and P. Ola Borjesson, "Low-complex frame synchronization in OFDM systems," in *Universal Personal Communications. 1995. Record., 1995 Fourth IEEE International Conference on*, Nov 1995, pp. 982–986.

[36] J. Davis and J. Jedwab, "Peak-to-mean power control in OFDM, Golay complementary sequences, and reed-muller codes," *IEEE Trans. Information Theory*, vol. 45, no. 7, pp. 2397–2417, Nov 1999.